Original Article

JOURNAL OF REINFORCED PLASTICS & COMPOSITES

Journal of Reinforced Plastics and Composites
2014, Vol. 33(22) 2064–2072

DOI: 10.1177/0731684414554635
jrp.sagepub.com

SAGE

Investigating the quasi-static puncture resistance of p-aramid nanocomposite impregnated with the shear thickening fluid

Hamid Reza Baharvandi[1], Peiman Khaksari[2], Morteza Alebouyeh[3], Masoud Alizadeh[4], Jalal Khojasteh[5] and Naser Kordani[5]

Abstract

The effect of impregnating p-aramid fabrics with shear thickening fluids on their quasi-static puncture resistance performance has been investigated. To prepare the shear thickening fluid, 12 and 60-nm silica particles have been dispersed in polyethylene glycol by means of mechanical mixing. The results of rheological tests indicate that the reduction of particle size leads to the increase of suspension viscosity, increase of critical shear rate, and the diminishing of the frequency of transition to elastic state for the shear thickening fluids. Samples of p-aramid impregnated fabrics were subjected to the quasi-static puncture resistance test according to the American Society for Testing and Materials standard D6264. The quasi-static puncture resistance increased 4.5 times for samples with 35 wt% silica concentration relative to the neat sample. In particular, with the reduction of particle size, the samples undergo less deformation and can withstand larger loads at each shear thickening fluid concentration. However, at low and medium concentrations (15 and 25 wt%), the reduction in the particle size has a large effect on the load-bearing capacity of the fabrics. But in the case of 35 wt% concentration for both the 12- and 60-nm particles, the difference between maximum loads withstood by the fabric is negligible.

Keywords

Shear thickening fluid, rheology, quasi-static puncture test, fabric–fluid nanocomposite, silica

Introduction

High-modulus and high-tenacity woven fabrics have been widely used as impact and puncture resistant products. However, they offer a limited level of protection against threats without reinforcement or coating. Recently, enhancing the performance of fabrics has been carried out with the addition of a reinforcer to the fabric to enhance the efficiency of the interaction of the yarns.[1] All related researches show that one way of improving the puncture resistance of high-modulus fabrics is to increase the friction between the fibers. By impregnating the fabrics with shear thickening fluids (STFs), a considerable increase in the puncture resistance with a little or no increase in the thickness or stiffness of these fabrics has been observed.[2–5]

[1]School of Metallurgy and Materials Engineering, University of Tehran, Tehran, Iran
[2]Ceramic Division, Department of Metallurgy and Materials Engineering, Iran University of Science and Technology, Tehran, Iran
[3]Department of Mechanical Engineering, Science and Research Branch, Islamic Azad University, Tehran, Iran
[4]Department of Textile Engineering, South Tehran Branch, Islamic Azad University, Tehran, Iran
[5]Department of Mechanical Engineering, Amir Kabir University of Technology, Tehran, Iran

Corresponding author:
Hamid Reza Baharvandi, School of Metallurgy and Materials Engineering, University of Tehran, Tehran 14395-515, Iran.
Email: baharvandi.h@gmail.com

Fluids can be divided into several classes in terms of their viscosity behavior with respect to shear rate. One of these classes is the Newtonian fluids, which exhibit a constant viscosity with the increase of shear rate.[6] Another class includes non-Newtonian fluids that exhibit a diminished viscosity with the increase of shear rate. These fluids are known as ''shear-thinning fluids.'' Another class of non-Newtonian fluids constitutes the STFs or dilatant fluids whose viscosity increases with the increase of shear rate.[7,8] When a considerable load applies from a foreign object to the STF, viscosity increases. The slope of viscosity increase in the thickening region is an important factor for STFs; the steeper this slope, the greater the energy absorbed from the foreign object.[9] The sudden increase of the STF viscosity with a very sharp slope is known as ''discontinuous thickening.''

To explain the underlying causes of the shear-thickening phenomenon, different theories have been formulated. The two theories of order–disorder transition and hydro-cluster formation give a better explanation of this behavior. The order–disorder transition theory attributes the shear-thickening phenomenon to the disorder in the arrangement of particles in the fluid caused by the application of shear rate. Conversely, the hydro-cluster hypothesis, attributes this phenomenon to the formation of hydro-clusters as a result of hydrodynamic forces overcoming the repulsive steric and Brownian forces.[7,10–12]

The shear-thickening phenomenon occurs in most of the concentrated colloidal suspensions containing hard solid particles.[13] This behavior has been observed in different fluid mixtures such as clay–water, calcium carbonate–water, polystyrene–silicon oil, iron particles–carbon tetrachloride, titanium oxide–resin, silica–polypropylene glycol, and silica–polyethylene glycol.[14]

The friction between the yarns and between the fibers and the penetrator greatly affects the puncture resistance of the fabric. During the penetration of a foreign object, the more friction there is between the yarns and between the fibers and the penetrator, the more rupture of fibers is observed relative to the slipping (sliding).[2] The enhancement provided by the STF in a STF/fabric composite is suspected to be due to the increased frictional interaction between the yarns.[15]

For a better understanding of the puncture mechanisms of the STF-treated fabric system, extensive testing and analysis are required. However, a quantitative analysis of nano-silica particle size on the quasi-static (QS) puncture performances of STF-coated p-aramid fabrics is not yet available in the open literature. The nanoparticle size of the STF is one of the dominant factors affecting shear-thickening phenomena and mechanical behavior of STF/fabric composite.[16,17]

Therefore, in this research, the effect of particle size on the rheological properties such as initial and final viscosities and the critical shear rate of fluids has been studied. Also, the effect of particle size on the QS puncture resistance and energy absorption of the p-aramid/STF composite has been analyzed at three different STF concentrations as 15%, 25%, and 35 wt%. The 15 wt% as the lowest concentration that shear thickening occurs and the 35 wt% as the highest concentration (close to saturation) that can be achieved in this kind of suspensions because the secondary purpose of this study is to demonstrate that the changes of rheological properties and puncture behavior by changing the particle size have a similar trend at each STF concentration.

Experimental procedures

Materials

Polyethylene glycol 200 g/mol (PEG200, Merck, Germany) was used as the continuous phase. Also, 12-nm silica particles (Evonik, Germany) as well as 60-nm silica particles (US Research Nanomaterials, Houston, USA) were used as dispersing phase in the polymer medium (PEG200).

The fabric used in this study was Twaron type D2200 with an areal density of 235 g/m^2. Twaron is a high-strength low-weight fabric with a plain weave made of p-aramid fibers.

Synthesis the STF samples

The STF samples were made with three different weight percentages of nanoparticles in the suspension (three different concentrations). For both particle sizes, 15, 25, and 35 wt% samples were prepared by dispersing the particles into the continuous phase using a 10-hp mechanical mixer rotating at 5700 r/min. The mixing continued until achieving a homogeneous and stable suspension. After preparing the suspension, it was left undisturbed at room temperature for 24 h in order to expel the air bubbles.

Preparation the p-aramid/STF composite

For a better infusion of the STF suspension into the fibers, the STF was diluted with absolute ethanol in proportions of 1:3 (STF:ethanol). The 152×152 mm^2 fabrics were soaked inside the STF–ethanol solution for 2 min and then were put under pressure by a 5-kg cylindrical roller. Afterward, the samples were placed in a drying oven for 25 min at a temperature of 60°C to drive out the added ethanol from the fabric and obtain the Twaron/STF composite. For both particle

sizes, the average weight of absorbed STF in the fabric at 15, 25, and 35 wt% samples were about 20, 24, and 27%, respectively.

Characterization and testing

The STF samples were tested for its rheological properties by the Anton Paar Phisica Rheometer-MCR 300. The shear rate sweep and frequency sweep test were performed on the samples. The diagrams of viscosity versus shear rate and dynamic modulus versus frequency were prepared. All the diagrams were obtained in the CP-50 mode (cone–plate geometry with a cone base diameter of 50 mm and apex angle of 1°).

The QS puncture tests were conducted based on the American Society for Testing and Materials standard D6264 by the INSTRON 1484 testing machine, at the speed of 6 mm/s. To apply the load on the $152 \times 152\,mm^2$ fabric, a steel Rounded edge penetrator with the diameter of 12.7 mm and length of 25 mm has been used. The QS puncture resistance of Twaron/STF composite fabrics has been examined.

Fabric is fixed between two steel frames with the thickness of 40 mm and length and width of 200 mm. In the center of the steel frames, there is a blank circular space with the diameter of 127 mm. The two frames are toughly joined together by four screws. In order to have no space left between the fabric and frames, an O-ring is used to prevent the fabric slippage during puncture test. Furthermore, boundary conditions of the fabric are considered to be completely fixed in all directions. Figure 1 shows the QS puncture test machine and the fabric being deformed during the test.

The images produced by the Philips XL30 scanning electron microscope have been used to observe the quality of impregnation of the fabrics with the STF.

Results and discussion

Rheological analysis

As can be observed in Figure 2, the shear rate sweep diagrams have been obtained for 15, 25, and 35 wt% STFs for both the 12 and 60-nm silica particles.

As shown in Figure 2, the diagram of the 15 wt% sample containing 12-nm silica particles has a constant viscosity of about 1.0 Pa.s, which indicates the Newtonian behavior of fluid at low shear rates.

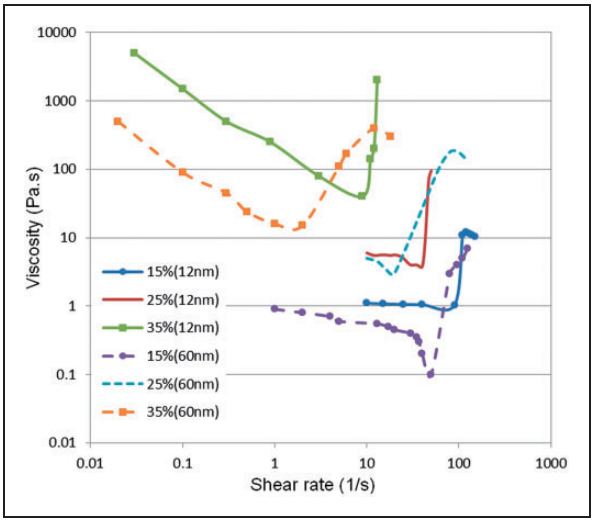

Figure 2. Shear rate sweep diagrams for 15, 25, and 35 wt% STFs for both the 12- and 60-nm silica particles.

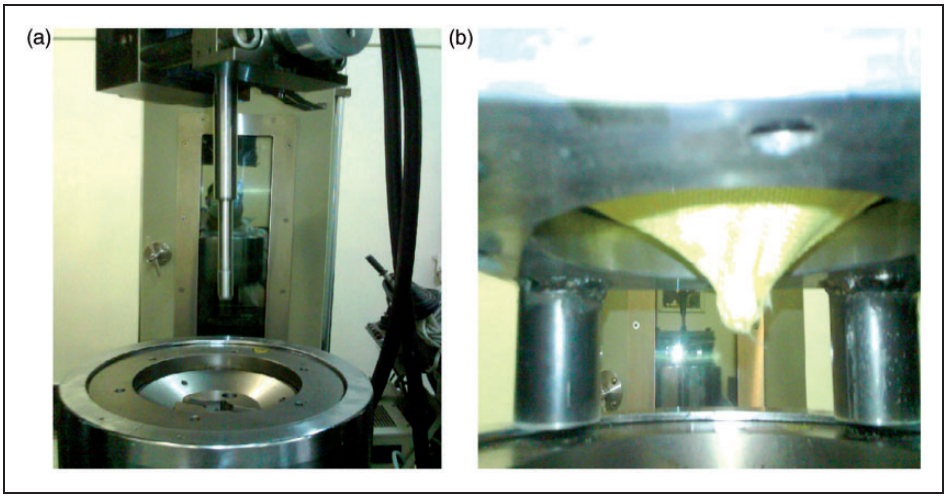

Figure 1. Quasi-static puncture test: (a) the INSTRON test machine and (b) deformed fabric during the test.

At the shear rate of 71 s^{-1}, a slight reduction of viscosity can be observed (shear thinning), and after the shear rate of 102 s^{-1} (critical shear rate), a sudden jump occurs in viscosity and it increases to about 10 Pa.s.

In the 15 wt% sample containing 60-nm silica particles, the initial viscosity is similar to that of the 12-nm sample, but at shear rates less than those of the 12-nm sample. With the increase of shear rate, viscosity diminishes with a steeper slope relative to the 12-nm sample. At the critical shear rate (63 s^{-1}), viscosity begins to increase with a milder slope relative to the 12-nm sample, which means the reduction of STF discontinuity.

In the 25 wt% sample containing 12-nm silica particles, the increase of viscosity begins at the critical shear rate of 55 s^{-1} and it rises from 6 Pa.s to about 100 Pa.s with a steep slope. At the shear rate of 24 s^{-1}, the viscosity of the 60-nm sample increases with a milder slope relative to the 12-nm sample.

In the 35 wt% sample containing 12-nm silica particles, it is initially observed that the viscosity is very high, but it diminishes gradually. At the critical shear rate (11 s^{-1}), the viscosity increases from 60 Pa.s to about 2000 Pa.s with a sharp slope. The 60-nm sample has a lower initial viscosity, its viscosity increases at a lower shear rate and with a milder slope.

Shear thinning, which is defined by a sudden drop in viscosity, occurs when the 3-D structures (hydro-clusters) that ordinarily exist in the suspension break down with the increase of shear rate and regular layers are formed, resulting in reduced viscosity and shear thinning. The viscosity drop is higher in the STFs containing larger particles because the bonds existing in the 3-D structures between the coarser particles and the polymer chains are weaker than those for finer particles.[18–21]

In the STF containing finer particles, because of a larger number of particles in the suspension, the increase in the effective volume fraction of solid component, more bonds are established between particles and polymer chains. Therefore, more hydro-cluster structures are formed. This means that, during the shear thickening phenomena, more hydro-cluster structures participate in increasing the viscosity; thus, the force transferring by the particles is easier to carry out. Consequently, the viscosity curve increases with a steeper slope. That is the reason for the sharper slope of viscosity increase in the shear-thickening region in the 12-nm sample relative to the 60-nm sample.

On the other hand, the increase of the particle size, due to the lowering of the surface repulsive forces reducing the polymer chains adsorbed to the particle surface and decreasing the Brownian forces cause the critical shear rate to diminish because a lower force of lubrication (resulting from shear rate) is needed to overcome the repulsive forces.[4,16,22] Moreover, as is observed in Figure 2, with the reduction of particle size, due to increasing of contacts between particles and fluid as well as more restriction in the movement of fluid layers relative to each other, the amount of viscosity increases.[10]

The frequency sweep diagrams of the 25 and 35 wt% samples at the frequency range of 0.1–100 rad/s have been illustrated in Figures 3 and 4, respectively.

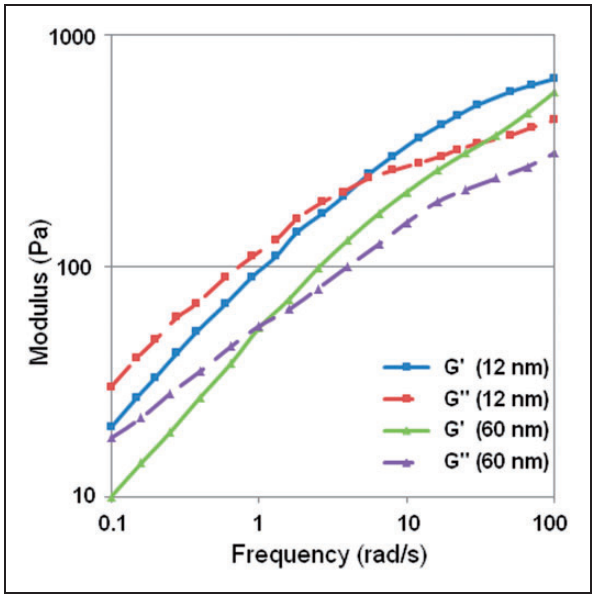

Figure 3. Frequency sweep diagrams of 25 wt% STFs for both the 12- and 60-nm silica particles.

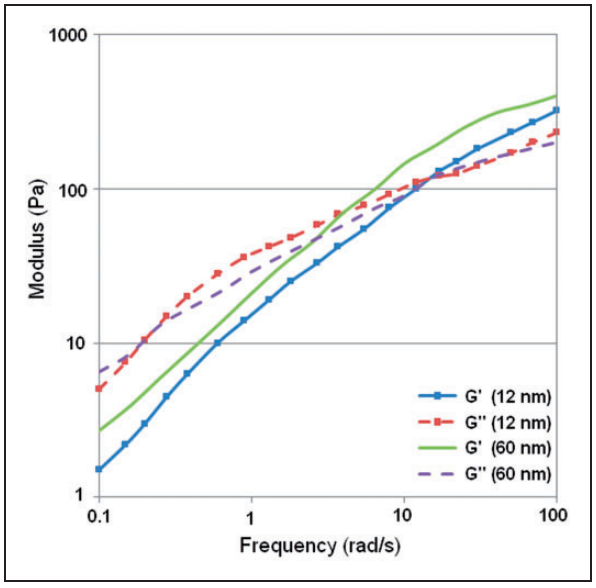

Figure 4. Frequency sweep diagrams of 35 wt% STFs for both the 12- and 60-nm silica particles.

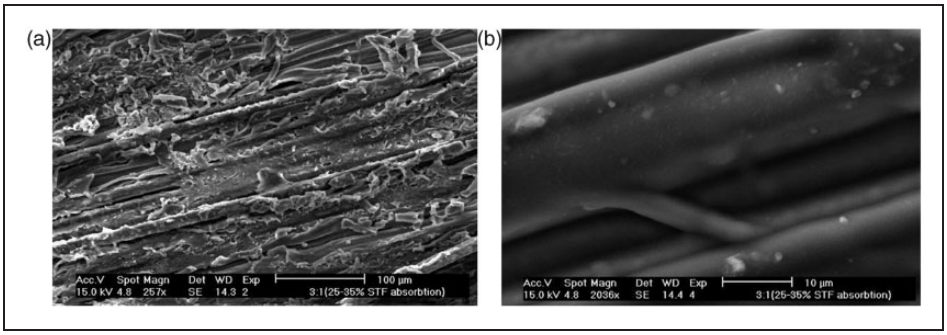

Figure 5. SEM images of the 25 wt% STF-impregnated Twaron containing 12-nm silica particles: (a) at 257 × magnification and (b) at 2036 × magnification.

The solid line and dashed line diagrams are associated with G' and G'', respectively. G' and G'' are dynamic modules obtained from dynamic rheological experiments in which G' and G'' are elastic modulus and loss modulus, respectively. The loss modulus indicates the gelatinous or pseudo-liquid behavior of the suspension; whereas, the elastic modulus characterizes its pseudo-solid behavior. Thus, when loss modulus G'' is higher than elastic modulus G', means that the viscous behavior of the fluid has prevailed over its elastic behavior and shows the suspension stability. When the G' curve is higher than the G'' one, means that connected lattice structures normally exist in the sample, and the sample has a solid-like or pseudo-elastic state. It should be mentioned that, the greater difference between G' and G'', means the greater magnitude of pseudo network in the suspension and thus the higher elastic contribution in the system.

The intersection point of G' and G'' curves is called the specific relaxation time (SRT). As Figure 3 shows, the increase of particle size leads to the reduction of transition frequency, SRT, from the viscous state to the elastic state. The SRT frequency indicates the onset of shear thickening.

In Figure 4, similar to Figure 3, with the increase of particle size, the SRT frequency diminishes. In Figures 3 and 4, it is observed that for all four samples at low frequencies, modulus G'' is higher than modulus G', which means that at low frequencies, the viscous behavior of the fluid has overcome to its elastic behavior.

In STFs with finer particles, the hydro-cluster aggregates form at higher angular frequencies. In other words, the fluid enters the elastic state with more delay; this means that the onset of shear thickening is postponed. This occurs because finer particles have larger Brownian and surface repulsive forces and need higher frequency for the formation of hydro-clusters and for prevailing the elastic behavior to the viscous state, which it means a better transmission of force in the suspension.[23]

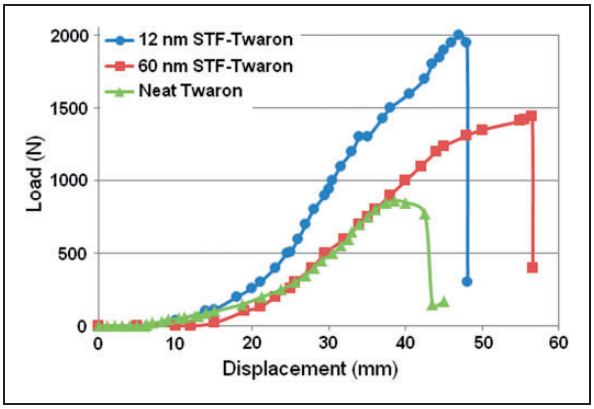

Figure 6. Load–displacement diagrams for the neat and the 15 wt% STFs-impregnated Twaron fabrics for both the 12- and 60-nm silica particles.

SEM images

The scanning electron microscope images of the 25 wt% STF-impregnated Twaron containing 12-nm particles have been illustrated in Figure 5. As the images show, the STF has been uniformly distributed into the yarns and fibers.

QS puncture tests

Figure 6 shows the QS puncture test diagrams of the neat and the 15 wt% STFs-impregnated Twaron fabrics for both the 12- and 60-nm silica particles. It is observed that, with adding STF, the load needed for puncturing the Twaron composite increases. All puncture test results have been obtained with five repetitions.

The maximum loads withstood by the neat and the 15 wt% STFs-impregnated Twaron fabrics for both the 12- and 60-nm silica particles were 863, 2001, and 1442 N, respectively. Also, the maximum displacements for the same samples were 43.2, 48.1, and 56.5 mm,

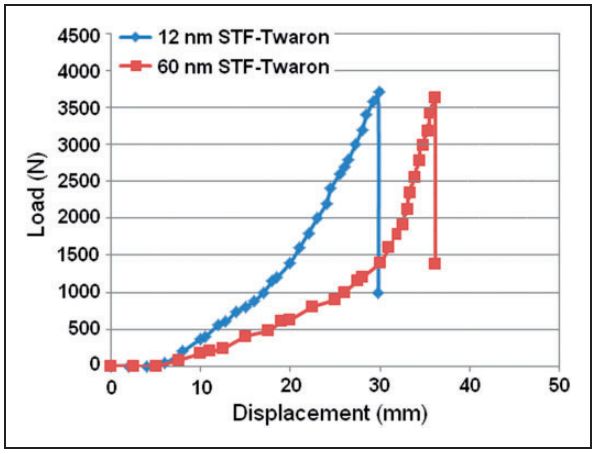

Figure 7. Load–displacement diagrams for the 25 wt% STFs-impregnated Twaron fabrics for both the 12- and 60-nm silica particles.

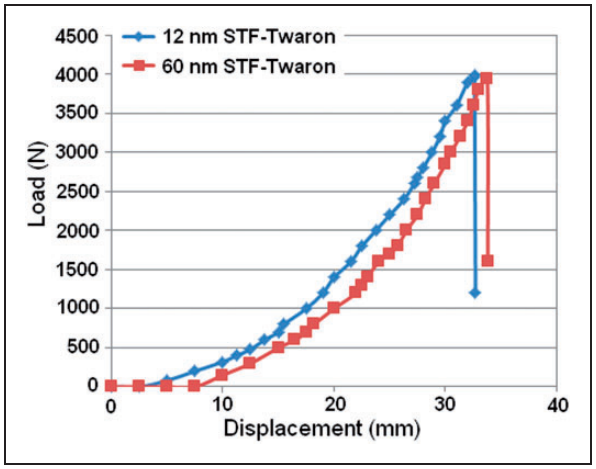

Figure 8. Load–displacement diagrams for the 35 wt% STFs-impregnated Twaron fabrics for both the 12- and 60-nm silica particles.

respectively. Maximum displacement means the largest deformation of the fabric before puncturing.

As the Figure 6 shows, the 15 wt% STF-impregnated Twaron containing the 60-nm particles punctures at a lesser load and greater displacement relative to that 12-nm sample. In the STFs-impregnated Twaron fabrics for both the 12- and 60-nm silica particles, the displacement that is caused by a specific load is less than the displacement that is produced by the same load in the neat sample because the STF-treated composite has more continuity, integrity, and uniformity compared to the neat fabric so that gaps between fibers and yarns are coated with the STF, which leads to a better stress distribution in the composite. Also, adding STF to the fabric generally restricts the motion of yarns and fibers relative to each other and better preserves arrangement and configuration of yarns and fibers.

In Figure 7, the load–displacement diagrams for the 25 wt% STFs-impregnated Twaron fabrics for both the 12- and 60-nm silica particles have been illustrated. According to the Figure 7, the increase of particle size has led to increase of displacement before yielding; while the maximum load withstood by the two samples has not changed by much. The 12- and 60-nm samples puncture at the loads of 3793 N and 3611 N and the displacements of 29.8 and 36.3 mm, respectively.

Figure 8 shows the diagrams of the 35 wt% STFs-impregnated Twaron fabrics for both the 12- and 60-nm silica particles. As is observed in the Figure 8, again the 60-nm sample exhibits more displacement relative to the 12-nm sample and the maximum loads tolerated by both samples are similar. The 12- and 60-nm samples puncture at the loads of 3983 N and 3934 N and the displacements of 32.6 and 33.7 mm, respectively.

The maximum absorbed energy of each sample was calculated by the area under the curve. The results of the Figures 6 through 8 along with the absorbed energy before puncturing have been summarized in Table 1.

When a penetrator exerts a load to a neat fabric, the fabric deforms and the produced strain is transferred along the fibers to the edges of the fabric. Due to the slow speed of the penetrator and because there is also a little friction between the fibers, they slip over each other and an opening form. Therefore, the penetrator easily passes through the fibers by puncture mechanisms including yarns and fibers sliding over each other, pushing aside them splitting of the yarn into separate bundles of fibers forming an opening (windowing) and pulling out (extraction) them.[24–26]

In the STF-treated fabric, based on the non-Newtonian and nonlinear reaction of the STF intercalated in the gaps between the fibers, the nanoparticles accumulate around the load application point and the STF viscosity heightens. The nonlinear increase of STF viscosity causes a considerable growth of friction between fabric and penetrator, between fibers themselves and between the yarns at their crossing points. This way, the fibers better keep their order and arrangement, and the penetrator encounters a higher resistance by the coated fabric when trying to push aside or pull out the yarns. In addition, relative to the untreated sample, more yarns participate in the pull out process and as a consequence, it becomes tougher to penetrate the fabric. Thus, in the STF-coated fabrics, compared to the neat fabric, puncture resistance or, in other words, energy absorption increases considerably.[24,26,27]

Shear thickening occurs even in QS loading. "The transitional behavior of a STF is fundamentally triggered by critical stress levels."[28] Normalizing the typical puncture force by penetrator tip surface area

Table 1. Maximum absorbed energy, load and displacement for the neat and 15, 25, and 35 wt% STFs-impregnated Twaron fabrics for both the 12- and 60-nm silica particles.

Samples	Max. displacement (m)	Max. load (N)	Max. absorbed energy (J)
Neat Twaron	43.2 E-3 ± 2	863 ± 8	14.3
15 wt%—12-nm STF/Twaron	48.1 E-3 ± 3	2001 ± 14	34.1
15 wt%—60-nm STF/Twaron	56.5 E-3 ± 4	1442 ± 9	32.4
25 wt%—12-nm STF/Twaron	29.8 E-3 ± 3	3793 ± 21	37.2
25 wt%—60-nm STF/Twaron	36.3 E-3 ± 2	3611 ± 12	34.3
35 wt%—12-nm STF/Twaron	32.6 E-3 ± 2	3983 ± 25	40.1
35 wt%—60-nm STF/Twaron	33.7 E-3 ± 2	3934 ± 16	35.2

provides tentative value of shear stress within the fabric of 10^6–10^7 Pa, high enough to induce transition (many orders of magnitude higher than the investigated STFs transitional stresses of ~10–10000 Pa). As a consequence, the stresses encountered by the STFs intercalated between the fibers are likely to be enough to trigger thickening.[28]

In explaining the effect of particle size, by examining the penetrator displacement during the full penetration process, it is realized that less deformation results from the finer particles in the STF; while larger particles lead to more deformation (Table 1). One reason is that the finer particles better distribute the energy. Furthermore, the applied load is converted to tensile forces in the fibers; in other words, the exerted load is spread over a larger area. The other reason is that the STF with coarser particles intercalated between the fibers has a smaller viscosity at all shear rate ranges compared to the STF with finer particles. Accordingly, the maximum-tolerated load and energy absorption of STF-impregnated fabrics with finer particles are more than those with coarser particles (Table 1).

As mentioned by comparing the STF-impregnated Twaron fabrics for both the 12- and 60-nm silica particles, it is observed that the 12-nm samples can withstand larger loads at each STF concentration. However, at low and medium concentrations (15 and 25 wt%), the reduction of particle size has large effect on the load-bearing capacity of the fabrics; while the case 35 wt% for both the 12- and 60-nm samples withstands almost the same loads. At low and medium concentrations due to the lower viscosity of STF, 12- and 60-nm samples behave quite differently in terms of the friction between fibers; i.e. the silica particle size considerably affects on the friction between fibers. At high concentrations, due to the high viscosity of both STFs, the friction difference resulting from the change of particle size is not noticeable and has a little effect on the load-bearing capacity of the fabric.[26–30] In other words, because of the high viscosity of high concentration STFs, changes of viscosity resulting from the change of the silica particle size are insignificantly in contrast to the high viscosity of each STF. Therefore, the maximum load bearing of these samples is almost the same.

Since Twaron fibers have a high breaking strength, the QS load needed for satisfying the failure criteria of fibers (fibers breakage) is higher than the required load for satisfying the criteria of puncture mechanisms because the friction between the fibers and yarns which is the unique criteria of puncture mechanisms in both the neat and treated sample is not as high as the breaking strength of Twaron fibers. Consequently, these puncture mechanisms play the role of the failure criteria of fabric in the QS puncture tests.

The QS puncture experiments performed in this study explore fabric puncture mechanisms that are naturally dependent on the effects of mobility of the yarn and filament. To study fabric defeat mechanisms including yarn and fiber compression or fiber shear and tensile failure, some other tests such as yarn pullout and ballistic penetration experiments are needed. It should be noted that these mechanisms can be broadly characterized as being dependent on either mechanical properties inherent to the yarn filaments or the effects of mobility of the yarn or filament. In other words, puncture mechanisms such as yarn sliding and windowing are most directly modified by restricting the ability of fibers and yarns to reorganize and move relative to each other. In contrast, compression, shear, and transverse failure are more directly related to the mechanical properties of the fabric filaments.[28]

Figure 9 depicts the pictures of punctured samples including untreated and 15, 25, and 35 wt% STFs-treated Twaron composites after the QS puncture tests.

As is evident in Figure 9, the puncture mechanisms including windowing, yarn pull out, etc. are observed in all the punctured samples. Also, no yarn breakage is seen. However, the manner the neat Twaron has been punctured indicates that the penetrator has created a larger opening with little yarn extraction in the fabric due to pushing aside most of the engaged yarns and

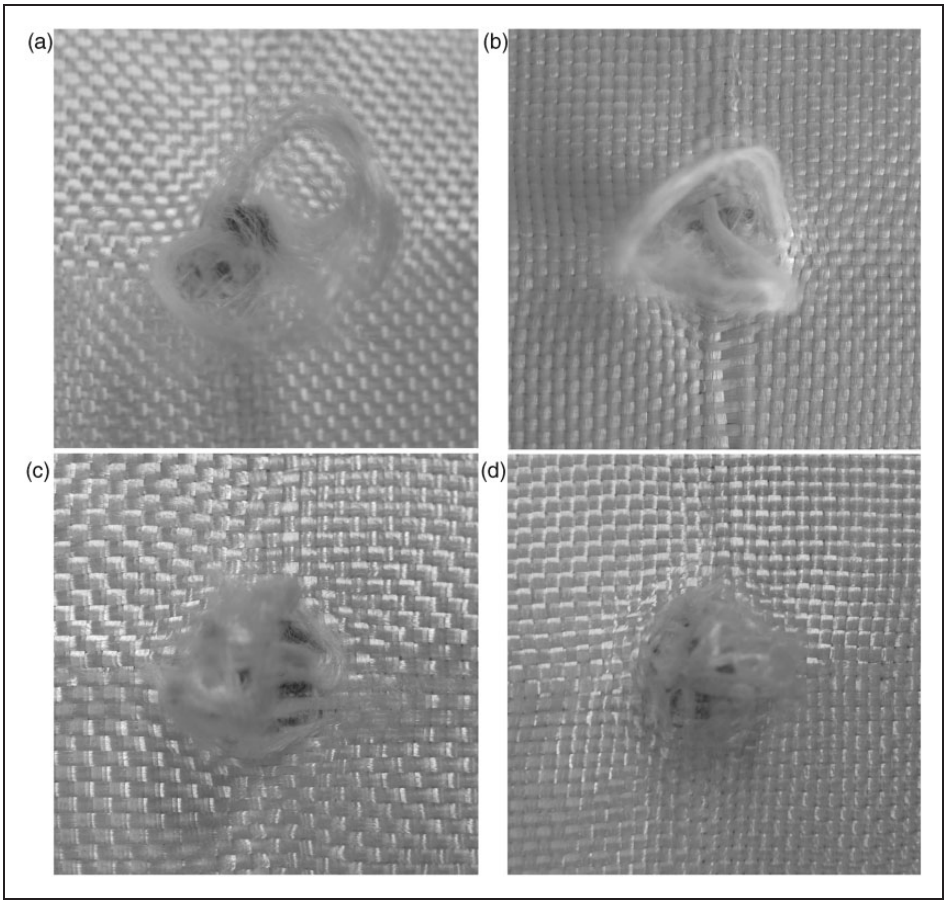

Figure 9. Pictures of punctured samples after the QS puncture tests: (a) neat Twaron; (b) 15% STF/Twaron composite; (c) 25% STF/Twaron composite; and (d) 35% STF/Twaron composite.

pulling out the rest of them; while in the Twaron/STF composites, more engaged yarns have participated in the puncture mechanisms because these mechanisms are most directly modified by restricting the ability of fibers and yarns to reorganize and move relative to each other.[28] In addition, with the increase of STF concentration, more extracted yarns are observed, the configuration of yarns and fibers is better preserved and the extracted fiber loops pulled out at the damage zone are becoming much smaller, which mean the improved puncture resistance and more energy absorption.

Conclusion

The findings of this paper can be summarized as the following conclusions:

1. The impregnation of Twaron fabric with STF significantly increases the QS puncture resistance so that in the 35 wt% STF-treated Twaron containing 12-nm particles, the tolerated load (3983 N) and the absorbed energy (40.1 J) increases almost 4.5 and 3 times relative to those for the neat Twaron (863 N and 14.3 J), respectively.
2. In the STFs, the reduction of particle size leads to the increase of suspension viscosity, critical shear rate, and transition frequency to elastic state (SRT frequency).
3. The reduction of particle size in the STF-treated Twaron fabrics leads to reduced deformation, increased maximum tolerated load, and increased energy absorption.
4. The changes of rheological properties and puncture behavior by changing the particle size have the similar trend at each STF concentration. For instance, the 12-nm samples can withstand larger loads at each STF concentration. However, at low and medium concentrations (15 and 25 wt%), the reduction in the particle size has a large effect on the load-bearing capacity of the fabrics; while in case 35 wt% STFs for both the 12- and 60-nm particles, the difference between maximum loads withstood by the composites is negligible.

Conflict of interest

None declared.

Funding

This research received no specific grant from any funding agency in the public, commercial, or not-for-profit sectors.

References

1. Lee BW and Kim CG. Computational analysis of shear thickening fluid impregnated fabrics subjected to ballistic impacts. *Adv Compos Mater* 2012; 21: 177–192.
2. Tan VBC, Tay TE and Teo WK. Strengthening fabric armor with silica colloidal suspensions. *Int J Solids Struct* 2005; 42: 1561–1576.
3. Srivastava A, Majumdar A and Butola BS. Improving the impact resistance performance of Kevlar fabrics using silica based shear thickening fluid. *Mater Sci Eng A* 2011; 526: 224–229.
4. Kalman DP, Schein JB, Houghton JM, et al. Polymer dispersion based shear thickening fluid-fabrics for protective application. In: *Proceedings of SAMPE*, Baltimore, MD, 3–7 June 2007, pp. 35–38.
5. Lomakin EV, Mossakovsky PA and Bragov AM. Investigation of impact resistance of multilayered oven composite barrier impregnated with the shear thickening fluid. *Arch Appl Mech* 2011; 81: 2007–2020.
6. Neagu CR, Bourban PE and Manson JAE. Micromechanics and damping properties of composites integrating shear thickening fluids. *Compos Sci Technol* 2009; 69: 515–522.
7. Astruc M and Navard PA. Flow-induced phase inversion in immiscible polymer blends containing a liquid-crystalline polymer studied by in situ optical microscopy. *J Rheol* 2000; 44: 4693–4712.
8. Krajnc A. *Shear thickening in colloidal dispersions*. Report. University of Ljubljana, Slovenia, 2011.
9. Bettin G. *Energy absorption of reticulated foams filled with shear thickening silica suspensions*. PhD Thesis, Massachusetts Institute of Technology, US, 2005.
10. Wetzel ED, Lee YS, Egres RG, et al. Novel flexible body armor utilizing shear thickening fluid (STF) composites. In: *14th International conference on composite materials*, San Diego, CA, July 2003, pp. 88–91.
11. Krieger IM and Dougherty TJA. Mechanism for non-Newtonian flow in suspensions of rigid spheres. *Trans Soc Rheol* 1959; 3: 137–152.
12. Rosales FJG, Hernandez FJR and Navarro JFV. Shear-thickening behaviour of Aerosil R816 nanoparticles suspensions in polar organic liquids. *Rheol Acta* 2009; 8: 334–341.
13. Barnes HA, Hutton JF and Walters K. *An introduction to rheology*. London: Elsevier Science Publishers, 1989, p.122.
14. Hassan TA, Rangari KV and Jeelani S. Synthesis, processing and characterization of shear thickening fluid (STF) impregnated fabric composites. *Mater Sci Eng A* 2010; 527: 2892–2899.
15. Duan Y, Keefe M, Bogetti TA, et al. Modeling friction effects on the ballistic impact behavior of a single-ply high-strength fabric. *Int J Impact Eng* 2005; 31: 996–1012.
16. Maranzano BJ and Wagner NJ. The effect of interparticle interactions and particle size on reversible shear thickening: hard sphere colloidal dispersions. *J Rheol* 2001; 45: 1205–1222.
17. Lee BW, Kim IJ and Kim CG. The influence of the particle size of silica on the ballistic performance of fabrics impregnated with silica colloidal suspension. *J Compos Mater* 2009; 43: 2679–2698.
18. Otsubo Y. Rheological behavior of suspensions flocculated by weak bridging of polymer coils. *J Colloid Interf Sci* 1999; 215: 99–105.
19. Auroy P, Auvray L and Linger L. Silica particles stabilized by long grafted polymer chains. *J Colloid Interf Sci* 1992; 150: 893–899.
20. Napper DH. Steric stabilization. *J Colloid Interf Sci* 1977; 58: 564–569.
21. Stenkamp VS and Berg JC. *The role of long tails in steric stabilization and hydrodynamic layer thickness*. London: Langmuir, 1997, p.3827.
22. Bergstrom L. Shear thinning and shear thickening of concentrated ceramic suspensions. *Colloids Surf A* 1998; 133: 151–155.
23. Lin YH, Ming RJ, Cheng ZZ, et al. Shear-thickening rheological response of PCC/PEG suspensions. *J Cent South Univ Technol* 2009; 16: 926–930.
24. Kang TJ, Hong KH and Yoo MR. Preparation and properties of fumed silica/Kevlar composite fabric for application of stab resistant material. *Fibers Polym* 2010; 11: 719–724.
25. Egres RG, Decker MJ, Halbach CJ, et al. Stab resistance of shear thickening fluids (STF)–Kevlar composites for body armor applications. In: *Proceedings of the 24th army science conference*, Orlando, FL, 29 November–2 December 2004, pp. 88–92.
26. Rao H, Hosur MV, Mayo J, et al. Stab characterization of hybrid ballistic fabrics. In: *Proceedings of the SEM annual conference*, Albuquerque, New Mexico, 1–4 June 2009, pp. 32–37.
27. Tomita M and Van De Ven TGM. *The structure of sheared ordered lattices*. Quebec: McGill University, 1983, p.77.
28. Kalman DP, Merrill RL, Wagner NJ, et al. Effect of particle hardness on the penetration behavior of fabrics intercalated with dry particles and concentrated particle-fluid suspensions. *ACS Appl Mater Interf* 2009; 1: 2602–2612.
29. Decker MJ, Halbach CJ, Nam CH, et al. Stab resistance of shear thickening fluid (STF)-treated fabrics. *Compos Sci Technol* 2007; 67: 565–578.
30. Alizadeh M. *Investigation on mechanical behaviours of hybrid woven fabrics with silica nanoparticles*. MSc Thesis, Islamic Azad University of South Tehran Branch, Iran, 2011.